

Tracking bacterial infection of macrophages using a novel red-emission pH sensor

Yuguang Jin · Yanqing Tian · Weiwen Zhang ·
Sei-Hum Jang · Alex K.-Y. Jen · Deirdre R. Meldrum

Received: 18 June 2010 / Revised: 20 July 2010 / Accepted: 21 July 2010 / Published online: 19 August 2010
© Springer-Verlag 2010

Abstract The relationship between bacteria and host phagocytic cells is key to the induction of immunity. To visualize and monitor bacterial infection, we developed a novel bacterial membrane permeable pH sensor for the noninvasive monitoring of bacterial entry into murine macrophages. The pH sensor was constructed using 2-dicyanomethylene-3-cyano-4,5,5-trimethyl-2,5-dihydrofuran (TCF) as an electron-withdrawing group and aniline as an electron-donating group. A piperazine moiety was used as the pH-sensitive group. Because of the strong electron-donating and -withdrawing units conjugated in the sensing moiety M, the fluorophore emitted in the red spectral window, away from the autofluorescence regions of the bacteria. Following the engulfment of sensor-labeled bacteria by macrophages and their subsequent merger with host lysosomes, the resulting low-pH environment enhances the fluorescence intensity of the pH sensors inside the bacteria. Time-lapse analysis of the fluorescent intensity suggested significant heterogeneity of bacterial uptake among macrophages. In addition, qRT-PCR analysis of the bacterial 16 S rRNA gene expression within single macrophage cells suggested that the 16 S rRNA of the bacteria was still intact 120 min after they had been engulfed by macrophages. A toxicity assay showed that the pH sensor has

no cytotoxicity towards either *E. coli* or murine macrophages. The sensor shows good repeatability, a long lifetime, and a fast response to pH changes, and can be used for a variety of bacteria.

Keywords Red emitter · pH sensor · Bacterial infection · Mouse macrophage

Introduction

Macrophages play important roles in controlling bacterial infection since they are one of the earliest of the host defense systems to become active [1]. The results of the interaction between bacteria and macrophages (i.e., survive or destroy) determine whether the infected hosts eventually develop the disease associated with the bacteria [2, 3]. To characterize interactions between the bacteria and macrophages, molecular tools are needed to track infection events (attachment, phagocytosis, and intracellular and extracellular killing) that occur between the addition of bacteria and the enumeration of surviving bacteria at different time points [1, 4, 5]. Attempts to do this have been made in the past few decades by performing the direct microscopic analysis of fixed samples [6, 7], by using engineered green fluorescence protein (GFP)-carrying bacteria for epifluorescent or confocal microscopic imaging [8, 9], or by utilizing fluorescent antibodies that can identify intracellular, attached, and freely suspended bacteria [10, 11]. However, applications of these methods are either limited by the snapshot nature of the analysis on fixed samples, the unavailability of genetically engineered bacteria, or the fact that antibody binding may alter the viability or receptor properties of bacteria [1]. An alternative approach is to label bacteria directly with fluorescence dye and then use them in infection studies. A variety of fluorescent stains have been developed with

Electronic supplementary material The online version of this article (doi:10.1007/s00216-010-4060-6) contains supplementary material, which is available to authorized users.

Y. Jin · Y. Tian (✉) · W. Zhang (✉) · D. R. Meldrum
Center for Ecogenomics, The Biodesign Institute,
Arizona State University,
PO Box 875801, Tempe, AZ 85287-5801, USA
e-mail: Yanqing.Tian@asu.edu
e-mail: Weiwen.Zhang@asu.edu

S.-H. Jang (✉) · A. K.-Y. Jen
Materials Science and Engineering, University of Washington,
Seattle, WA 98195-2120, USA
e-mail: jangsh@u.washington.edu

different binding characteristics, such as fluorescein-derived dyes for covalent protein binding or Hoechst 33258, lipophilic dye PKH-2, chromomycin A3, and acridine orange for nucleic acid binding [1, 3, 12]. However, acridine orange and Hoechst dyes are known to be cytotoxic to prokaryotic and eukaryotic cells, and PKH-2 is nontoxic in the dark but toxic under conditions of light irradiation [13].

Although the molecular mechanism of bacterial survival in macrophages is still not fully elucidated, one major killing mechanism of macrophages has been proposed to be the acidification of pathogen-containing phagosomes to $\text{pH} < 5.0$, under which conditions the activity of lysosomal enzymes is optimal and the survival rates of many bacteria are diminished [2, 3, 14]. In turn, bacteria have developed various strategies to counteract host cell assaults, such as escaping from the phagosome into the cytoplasm, inhibiting phagosome acidification, an absence of phagosome–lysosome fusion, and adapting acidic phagolysosomes, which eventually leads to survival and multiplication in macrophages [15, 16]. In most of these processes, the fate of the bacteria is dependent on the change in pH of their local environments inside cells, which makes intercellular pH sensors good agents for tracking bacteria–host interactions during phagocytosis. Although many pH sensors are suitable for intracellular pH measurements of eukaryotic cells, such as 2',7'-bis-(2-carboxyethyl)-5 (and 6)-carboxyfluorescein (BCECF) [17], carboxy-seminaphthorhodafluor-1 (C-SNARF-1) [18], and silica and polymer particles [19] with suitable fluorophores, these are not suitable for bacteria due to either the pK_a mismatch, a high rate of passive leakage from the cells, or the fact that the materials cannot be up taken by bacterial cells. Thus, sensors that can react with certain functional groups of bacteria were developed in order to avoid the efflux of the sensors from the bacteria [3]. However, chemical modification of the bacteria may lower or alter their bioactivities.

Herein, we report the synthesis of a novel pH sensor for the real-time monitoring of bacterial infection and its application to monitor the early events of *Escherichia coli* infection using

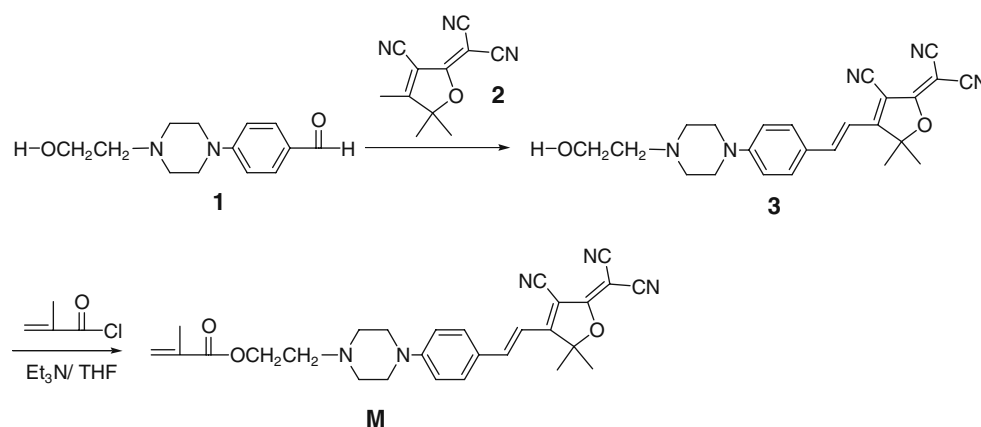
a murine macrophage model system. The pH sensor was constructed using 2-dicyanomethylene-3-cyano-4,5,5-trimethyl-2,5-dihydrofuran (TCF) as an electron-withdrawing group and aniline as an electron-donating group (M, Scheme 1). A piperazine moiety was used as the pH-sensitive group. Because of the strong electron-donating and -withdrawing units conjugated within the sensing moiety, M, the fluorophore emits in the red spectral window. A red emitter is preferred because the red spectral window minimizes effects resulting from the natural fluorescence of bacterial cells. The electron acceptor TCF has been widely studied and used in nonlinear optical materials [20–22]. Here, for the first time, we used this acceptor as an electron-withdrawing group to create a new pH-sensitive red emitter, M. This material was shown to be able to permeate through bacterial (herein *E. coli* and *Bacillus*) membrane. Following the engulfment of sensor-labeled bacteria by murine macrophages and their subsequent merger with host lysosomes, the resulting acidic environment enhanced the fluorescence intensity of the probe in the bacteria due to the protonation of the amino group of the probe, which facilitates fluorophore emission by inhibiting photoinduced electron transfer (PET). This makes the pH sensor a highly sensitive fluorescent probe for tracking bacteria–host interactions during the phagocytosis process. On the other hand, the fluorophore is also a monomer that possesses a methacrylate unit, meaning that it has great potential for further application in polymer science.

Materials and methods

Chemicals

Compounds 1 and 2 were prepared according to previous reported procedures [23–26]. Triethyl amine (Et_3N), tetrahydrofuran (THF), methacryloyl chloride and trypan blue were purchased from Sigma Aldrich (St. Louis, MO, USA) and used without further purification. 4',6-Diamidino-2-

Scheme 1 Synthesis of the pH sensor M



phenylindole (DAPI) was obtained from Sigma Aldrich and lysosensor green from Invitrogen (Carlsbad, CA, USA).

Synthesis of the pH sensor M

i) *Synthesis of compound 3*. A mixture of compound 1 (0.234 g, 1.0 mmol), TCF acceptor 2 (0.200 g, 1.0 mmol), and ammonium acetate (0.077 g, 1.0 mmol) were dissolved in a mixture of 1 mL of THF and 1 mL of ethanol. The mixture was stirred for 8 h at room temperature. Filtration gave a black solid, which was further washed using ether to get compound 3. The yield was 0.21 g (51%). ^1H NMR (300 MHz, CDCl_3 , δ , ppm): 7.62 (1H, d, $J=16.4$ Hz), 7.57 (2H, d, $J=8.8$ Hz), 6.92 (2H, d, $J=8.8$ Hz), 6.82 (1H, d, $J=16.4$ Hz), 3.72 (2H, t, $J=6.0$ Hz), 3.50 (4H, t, $J=5.6$ Hz), 2.71 (2H, t, $J=6.0$ Hz), 2.65 (4H, t, $J=5.6$ Hz), 1.79 (6H, s). ^{13}C NMR (125 MHz, CDCl_3 , δ , ppm): 176.18, 174.42, 154.12, 147.96, 132.07, 123.77, 114.30, 112.55, 111.80, 111.30, 110.32, 97.22, 95.93, 59.47, 58.03, 55.69, 52.58, 47.11, 26.88. EI-HRMS: m/e calculated for $\text{C}_{24}\text{H}_{26}\text{N}_5\text{O}_2$ (M+H) 416.2081, found 416.2077.

ii) *Preparation of M*. Compound 3 (520 mg, 1.25 mmol) and 1 mL Et_3N were dissolved into 10 mL of THF, and then 150 mg of methacryloyl chloride (1.43 mmol) was added dropwise. The mixture was stirred at room temperature overnight. After the solvent had been removed, the residue was passed through a column chromatograph using CH_2Cl_2 as the eluent. Yield: 320 mg (53%). ^1H NMR (300 MHz, CDCl_3 , δ , ppm): 7.62 (1H, d, $J=16.4$ Hz), 7.57 (2H, d, $J=8.8$ Hz), 6.88 (2H, d, $J=8.8$ Hz), 6.79 (1H, d, $J=16.4$ Hz), 6.12 (1H, s), 5.60 (1H, s), 4.34 (2H, t, $J=6.0$ Hz), 3.47 (4H, t, $J=5.6$ Hz), 2.77 (4H, t, $J=5.6$ Hz), 2.70 (2H, t, $J=5.2$ Hz), 1.97 (3H, s), 1.77 (6H, s). ^{13}C NMR (125 MHz, CDCl_3 , δ , ppm): 176.26, 174.50, 167.45, 154.20, 148.12, 136.37, 132.16, 125.90, 123.61, 114.21, 112.64, 111.89, 111.37, 110.13, 97.25, 95.60, 62.30, 56.65, 55.41, 52.99, 47.04, 26.87, 18.53. EI-HRMS: m/e calculated for $\text{C}_{28}\text{H}_{30}\text{N}_5\text{O}_3$ (M + H) 484.2343, found 484.2333.

Characterization of pH sensor M

^1H NMR spectra were measured using a Bruker 300 spectrometer operating at 300 MHz. ^{13}C NMR spectra were measured using a Bruker 500 spectrometer operating at 125 MHz. High-resolution mass spectrometry (HRMS) was performed by the University of Washington's Biological Mass Spectrometry Lab. UV-Vis absorption spectra were measured using a Shimadzu UV-3600 UV-vis-NIR spectrophotometer. Fluorescence spectra were recorded with a Shimadzu RF-5301 spectrofluorophotometer. Fluorescence quantum yields were obtained by comparing the integrated

fluorescence spectra of the polymers in solution to the fluorescence spectrum of rhodamine in ethanol ($\Phi=0.65$) [27], correcting for refractive index differences. Titrations were performed in Britton–Robinson (B–R) buffers consisting of acetic acid, boric acid, phosphoric acid, and sodium hydroxide. The cytotoxicity of the sensor to bacteria and mouse macrophages was measured by incubating a high concentration of the sensor with bacteria and macrophages for certain period of time and then calculating the survival rates.

Cultivation of bacteria and murine macrophages

Escherichia coli and *Bacillus* sp. cells were cultivated in LB medium and collected during the mid-exponential phase [28]. The pH sensor, M, was first dissolved in dimethyl sulfoxide (DMSO) solution and diluted with LB medium to a final concentration of 3 μM , and then incubated with bacterial cells for 30 min in a shaker (150 rpm) at 37 °C. Murine macrophage RAW 264.7 cells (American Type Culture Collection, Manassas, VA, USA) were cultured in Dulbecco's Modified Eagle's Medium (DMEM) supplemented with 10% fetal bovine serum (FBS) and incubated at 37 °C in a 5% CO_2 atmosphere. The cells were seeded in 35 mm glass-bottom culture dishes (MatTek Crop, Ashland, MA, USA) at 10,000–50,000 cells/mL for a total of 2 mL and incubated for 2–16 h before cell infection.

Effects of pH sensor M on the bacteria

E. coli and *Bacillus* sp. cells were cultivated and collected during the mid-exponential phase. The pH sensor was added to the *E. coli* and *Bacillus* sp. cultures in LB medium at final concentrations of 0.3 μM to 3 μM , and then incubated at 37 °C in a shaker (150 rpm) for 30 min to 20 h. The environmental pH was adjusted to pH 7.0. The sensor-labeled cells from different pH treatments were then loaded onto slides for microscopic examination using a Nikon TE2000-E C1si confocal microscope. The images were taken by using a triple stain combination of lasers and filters, including a violet laser (405 nm), an argon laser (488 nm), and a HeNe laser (543 nm). The combination filter sets were DAPI, FIFC and TMR. Emission filters were 450/35 for blue fluorescence, 515/30 for green fluorescence, and 605/75 for red fluorescence. Negligible background cell fluorescence was detected under the settings used.

Viable macrophage cell counting using trypan blue

Using the typical staining procedure of trypan blue, 0.4% trypan blue stain was added in a 1:1 ratio to the cell culture medium (100 mL) with eukaryotic cells in a 24-well culture plate with 100,000 cells/ml that had internalized the sensors for 30 min, 3 h, 7 h and 24 h,

and the stain and medium were mixed thoroughly. After standing for 5 min at room temperature (22 °C), the cells were imaged using an optical microscope in bright field mode. Dead cells appear blue when they are stained, while healthy cells appear transparent due to their resistance to being stained. Cells were counted and the ratio of dead cells to live cells was calculated. Each experiment was repeated three times.

Bacterial transfection

The pH sensor loaded *E. coli* cells were washed three times in phosphate buffer (PBS, pH 7.0) and vortexed to disrupt aggregates. These cells were then added to macrophages with a multiplicity of infection (MOI) of 10–50 after imaging the uninfected macrophage for 85 s. The infected macrophages were then monitored for another 20–30 min.

Time-lapse confocal imaging

Live cells were imaged and recorded in a time-lapse video recorded with a Nikon TE2000-E C1si confocal microscope for 20–30 min, with each frame corresponding to 12–15 s. A laser with an excitation wavelength of 488 nm was used, and the emission was collected from 579 to 673 nm. Negligible background cell fluorescence was detected with the settings used.

qRT-PCR analysis of bacterial transfection in single macrophage cells

About 2, 20 and 120 min after the infection of mouse macrophages by the pH sensor M loaded *E. coli*, single macrophage cells were selected using a robotic single-cell manipulation system developed in our research center [29], which can aspirate a single cell in a total volume of 50 nL and delivered it into a 100 µL PCR tube (Applied Biosystems, Foster City, CA, USA) containing 100 µl of RNA lysis buffer from a ZR RNA MicroPrep Kit (Zymo Research, Orange, CA, USA). RNA extraction from the single cell was carried out using ZR RNA MicroPrep Kit (Zymo Research), following the manufacturer's instructions. A total of 5 µL of RNA were eluted from the column matrix and immediately used or stored at –80 °C. A SuperScript VILO cDNA Synthesis Kit (Invitrogen) was used for cDNA synthesis. cDNA synthesis was performed in a total volume of 10 µL comprising the following: 2 µL of 5× VILO Reaction Mix, 1 µL of 10× SuperScript Enzyme Mix, 5 µL of total RNA from a single cell, as well as 2 µL of DEPC-treated water (Ambion, Austin, TX, USA). After gently mixing the tube contents and incubating at 25 °C for 10 min, the cDNA synthesis was performed at 42 °C for 60 min

followed by 85 °C for 5 min to inactivate reverse transcriptase. Diluted or undiluted cDNA was used in the qPCR immediately. Primer 3 software (available online) was used for 16 S rRNA primer design. The PCR primers for the 16 S rRNA gene were 16 S rRNA-F: 5'-GTTAATACCTTTGCT CATTGA-3' and 16 S rRNA-R: 5'-ACCAGGGTATC TAATCCTGTT-3'. Primer effectiveness and efficiency were initially validated in bulk cells before they were selected for use in single-cell analysis. An EXPRESS SYBR GreenER qPCR SuperMix Kit (Invitrogen) was used for qPCR analysis. In a 0.1 mL PCR tube (Applied Biosystems, Foster City, CA, USA), the qPCR reaction was performed in a total volume of 10 µL comprising the following: 5 µL of EXPRESS SYBR GreenER qPCR SuperMix Universal, 1 µL of each primer (4 µM), 0.1 µL of ROX Reference Dye (25 µM), 1 µL of diluted or undiluted cDNA, as well as 2.9 µL of DEPC-treated water. The thermal cycling program applied on the ABI StepOne was: 95 °C for 5 min, 40 cycles of 95 °C for 15 s, 60 °C for 1 min, 80 °C for 10 s (for signal detection), followed by a melting curve analysis performed using the default program of the ABI StepOne qPCR machine (Applied Biosystems). Data analysis was carried out using the software provided by Applied Biosystems Inc.

Results

Synthesis and in vitro characterization of the pH sensor M

The pH sensor, M, showed a good pH response in B–R buffer. Typical UV-vis and fluorescence spectral changes at various pH values are shown in Fig. 1A, B. Under neutral and basic conditions, the absorbance curve is very broad. This may be related to chromophore aggregation, as it exhibits low water solubility under neutral and basic conditions. When the pH was lowered to <7.0, the spectra became sharper. This change is most likely due to the fact that the fluorophore has better water solubility after the amino group has been protonated. An isosbestic point was observed at 528 nm, showing that the sensor responds to pH through a single acidification and basification mechanism. Because of the aggregation of the fluorophores under neutral and basic conditions, the emission maxima occurred at approximately 640 nm. When the pH was lowered to <7.0, the maxima shifted to 617 nm and the emission intensity significantly increased as the pH decreased. The emission intensity at 617 nm enhanced 7.5-fold when the fluorophore was excited at 528 nm. The change in emission intensity was sigmoidal (Boltzmann fitting):

$$\frac{F}{F_0} = \frac{m_1 - m_2}{1 + \exp\left(\frac{pH - pK'_a}{p}\right)} + m_2, \quad (1)$$

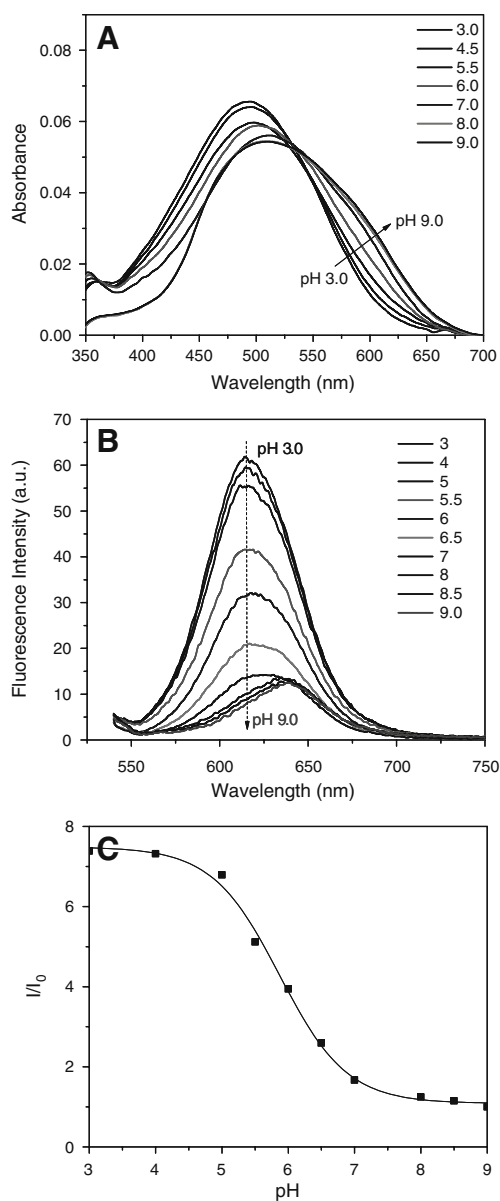


Fig. 1 pH response of the sensor M in B-R buffer. **A** Absorbance changes, **B** emission intensity changes after excitation at 528 nm, **C** sigmoidal plot of the intensity ratio of I/I_0 . I is the emission intensity at 617 nm for various pH values, while I_0 is the emission intensity at 617 nm at pH 9.0

where F and F_0 are the fluorescence intensities at 617 nm measured at various pH values and at the highest pH value (pH 9.0) used during the titration, respectively. m_1 , m_2 , pK_a' , and p are empirical parameters that describe the initial value (m_1), the final value (m_2), the point of inflection (pK_a'), and the width (p) of the sigmoidal curve. The changes in fluorescence intensity and their curve fits are shown in Fig. 1C. The apparent pK_a value (pK_a') was 5.86, with a correlation coefficient of 0.995.

The fluorescence intensity changes were ascribed to the suppression of photoinduced electron transfer (PET)

in the pH sensor due to the protonation of the amino group. When a fluorophore is attached to an electron quencher (usually one or more nitrogen-containing functional groups that are not conjugated to the fluorophore), PET occurs between them (Fig. 2) [30–34]. In the piperazinyl group of M, the nitrogen atom in NCH_2CH_2 is not directly connected to the TCF-conjugated fluorophore, although the NCH_2CH_2 moiety is a strong electron donor to this fluorophore. PET occurs from the lone electron pair of the amine group to the acceptor TCF-containing fluorophore, making the sensor only weakly fluorescent. At low pH values, however, the protonation of the amino group diminishes the PET effect, thus causing a restoration of fluorescence from the fluorophore. Hence, a remarkable increase in emission intensity was observed at low pH.

Staining of various bacteria and macrophages by the pH sensor M

To demonstrate the utility of the newly synthesized pH sensor for intracellular measurements, we first tested the permeability of the sensor through the membranes of various bacterial cells and murine macrophages. Confocal microscopic analysis showed that, after incubating them with the sensor for 20–30 min at room temperature, *E. coli* and *Bacillus* sp. cells had absorbed a significant amount of the sensor. Washing with LB medium or PBS three times did not decrease the fluorescence, suggesting that the sensor is intracellularly stable (Fig. 3). Not much difference was observed in terms of sensor absorption between *E. coli* and *Bacillus* sp., suggesting that the sensor could potentially be used to label different bacterial species. Typical fluorescence spectra of M inside *E. coli* are shown in Fig. 3E, F. The emission peak at ~623 nm indicates that the intracellular pH value of *E. coli* lies between 7.0 and 8.0 (Fig. 1b), which is in accordance with the reported neutral or slightly basic intracellular pH environment of *E. coli*. The red emission is clear apparent under the confocal fluorescence microscope, and it is much stronger than the background autofluorescence of the bacteria. This observation coincides with our consideration of the development of a red emitter for reducing the autofluorescence of biospecimens. The sensor can also be absorbed by murine macrophages after 20 min of incubation at room temperature. To determine the subcellular distribution of the sensor inside macrophage cells, we stained the macrophage cells with DAPI (which stains the cell nucleus) and lysosensor green (which stains acidic organelles such as lysosomes, which have a pH range of 4.5–5.0). The overlaid image showed that the M sensor stained mainly lysosomes, consistent with its ability to stain acidic organelles (Fig. 4). This shows that it is a new red emitter lysosensor. Most likely, the amino groups are

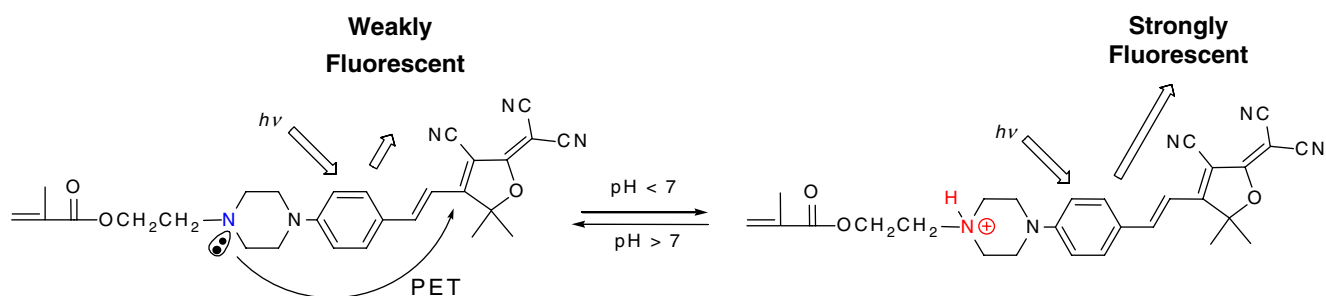
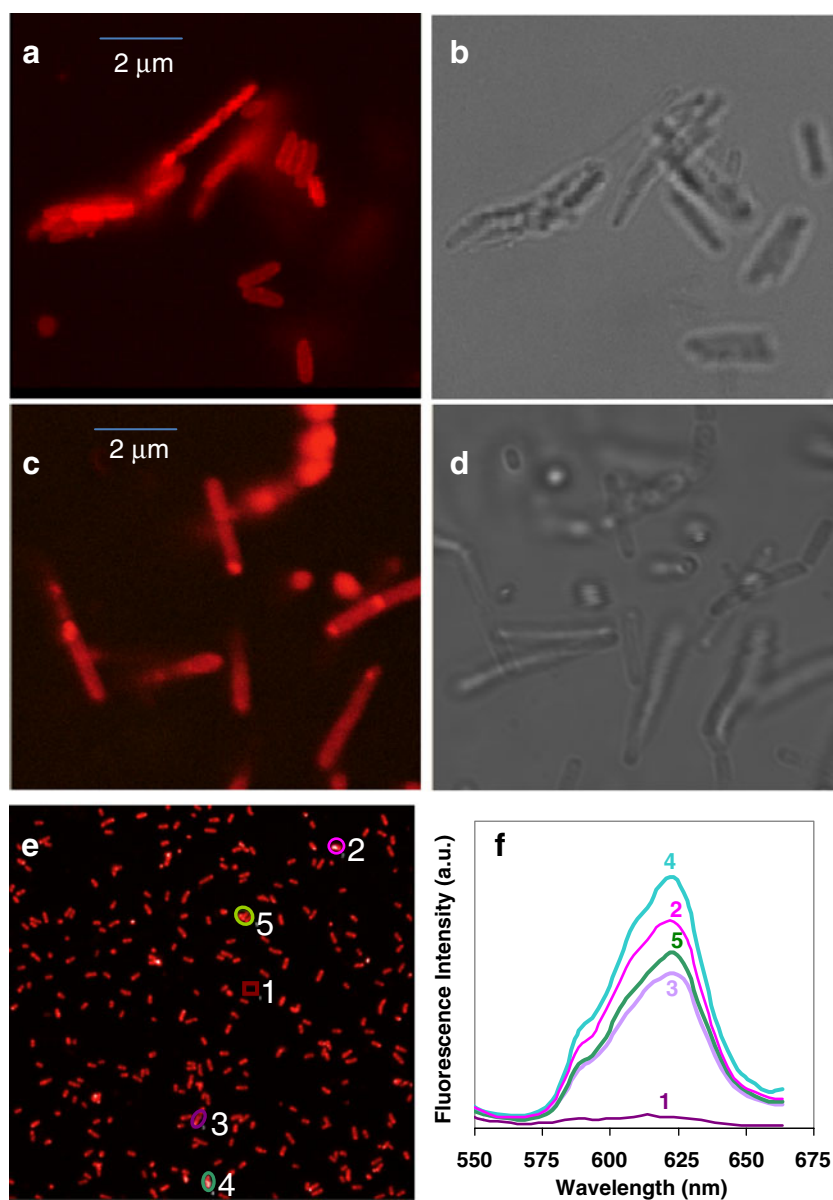


Fig. 2 Mechanism of the pH response, which is related to the PET mechanism

protonated by lysosomes of the macrophage cells, which suppresses the fluorescence quenching of the TCF-conjugated fluorophores caused by the amino groups. The protonated amino groups enable the selective accumulation of the probes in the acidic organelles [12].

To determine the effects of sensor M labeling on bacteria and macrophages, labeled and unlabeled *E. coli* and macrophage cells were standardized spectrophotometrically and compared on the basis of recoveries on both solid and liquid media. Three different sensor concen-

Fig. 3 Confocal fluorescence images of *E. coli* with the pH sensor. **A** Confocal fluorescence image of *E. coli* loaded with the sensor M. Bar: 2 μm . **B** Bright-field image of *E. coli* loaded with M. **C** Confocal fluorescence image of *Bacillus* sp. loaded with M. Size: 2 μm . **D** Bright-field image of *Bacillus* sp. loaded with M. **E** Large-area fluorescence images of M in *E. coli*. **F** Spectrometric analysis of the image shown in **E**. Spot 1 represents fluorescence from the background. Spots 2, 3, 4 and 5 represent spectra from four selected areas in image **E**



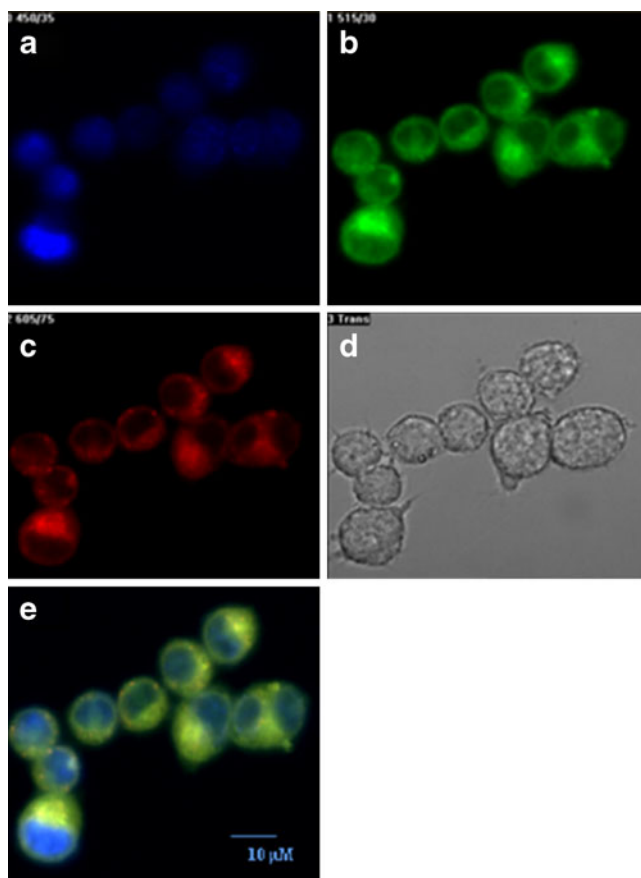


Fig. 4 Confocal fluorescence images of murine macrophage RAW 264.7 with **A** DAPI staining; **B** lysosensor green staining; and **C** pH sensor M staining. **D** The bright-field image. **E** The overlaid image of **A**, **B** and **C**. Bar: 10 μm

trations (0.3 μM , 3 μM and 30 μM) were used, although the typical concentration we used for bacterial cell labeling was 3 μM . The results showed that the growth of macrophage cells was not affected by incubation with sensor M for 30 mins (see the “[Electronic Supplementary Material](#),” Fig. S1). We also investigated the growth time-courses of *E. coli* with and without 0.3 μM or 3 μM dye. The results showed no significant growth differences during growth for 20 h overnight based on cell density measurements. Similarly, we used different sensor concentrations (i.e., 0 as a control, 0.3 μM , 3 μM and 30 μM), and performed macrophage incubations for different time periods (i.e., 30 min, 3 h, 7 h and 24 h). The trypan blue viable cell counting method was used to determine cell death after each treatment. The results showed that virtually none of the cells had died after 7 h of incubation with 3 μM sensor, and only 30% of the cells had died after 24 h of incubation with 3 μM sensor. When the sensor concentration was increased tenfold to 30 μM , again, virtually none of the cells died after 3 h of incubation, and only 15% of the cells died after 7 h of incubation with 30 μM dye (see the “[Electronic Supplementary Material](#),”

Fig. S2). These results suggest that pH sensor M is nontoxic to both bacteria and macrophage cells under the experimental conditions employed and are thus suitable for intracellular pH measurements.

Time-lapse confocal imaging of bacterial transfection into macrophages

Time-lapse confocal microscopy was previously used to monitor the development of GFP carrying *B. anthracis* spores inside macrophages over time. This method overcame some of the limitations of using “snapshot” views of fixed specimens, since it allows better tracking of the life histories of individual fluorescent spores [9]. Therefore, to investigate the engulfment of bacteria by macrophages in real time, we applied time-lapse confocal microscopy to follow individual macrophages over time. In our experiment, macrophage cells were infected with the pH sensor loaded *E. coli* and then fluorescence images from the pH sensor M were measured over time. The results showed that the engulfment of bacteria by macrophages occurred only 2 min after the bacteria had been added to the macrophage cells, and the highest fluorescent intensity of M was observed after 15 min (Fig. 5), suggesting that the uptake of bacteria by macrophages is a very fast biological process. Recall that the sensor’s emission peak inside neutral *E. coli* is ~ 623 nm. The sensor’s emission peak shifted to ~ 618 nm inside the macrophage RAW 264.7 cells after the transfection, indicating that the sensors are located in the acidic lysosome compartment. The sensor is not ratiometric, making it difficult to measure the exact pH_i of the macrophage cells. However, the difference in emission peaks between the sensor inside *E. coli* and the sensor inside macrophages indicates that the sensor is a qualitative intracellular pH indicator that can be utilized as a new lysosensor, as discussed before.

Although the general patterns were similar for all macrophage cells, the time-lapse confocal image analysis also revealed that the increase in fluorescent intensity was not uniform for all of the macrophage cells observed, suggesting a high degree of heterogeneity in terms of speed and/or number of bacteria engulfed by each of the macrophages (Fig. 5). The results also demonstrate that the pH sensor is a good analytical tool for real-time analysis of cell heterogeneity.

Validation of bacterial transfection by single-cell qRT-PCR

To confirm that the fluorescent intensity increase does indeed result from bacterial engulfment, we selected individual macrophages throughout the time course of infection using a robotic single-cell manipulation system. Each individual macrophage, after washing it three times

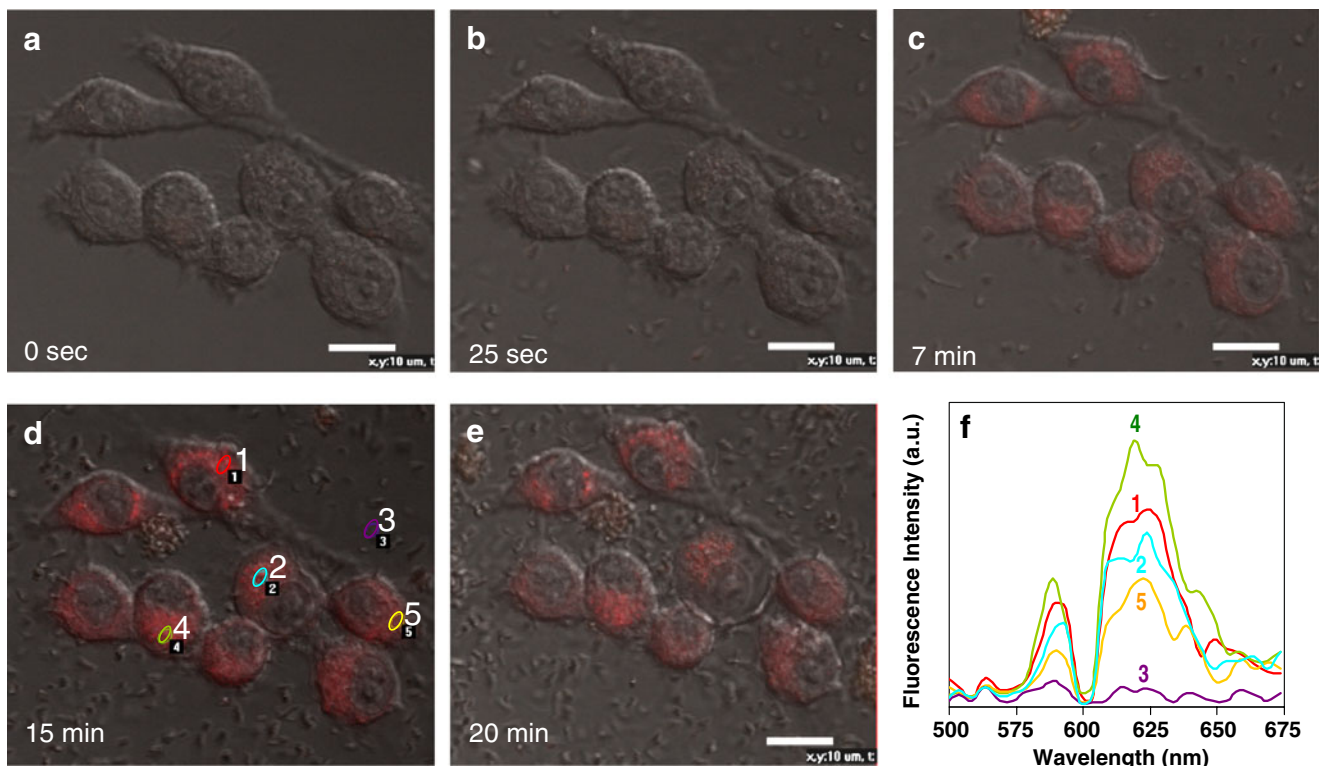


Fig. 5 Time-lapse confocal image analysis of bacterial infection of murine macrophage RAW 264.7. **A** 0 s, before infection; **B** 25 s; **C** 7 min; **D** 15 min; **E** 20 min after bacterial infection. **F** Spectral analysis

of the sensor in macrophages 15 min after being infected by *E. coli*. Spot 3 represents fluorescence from the background. Spots 1, 2, 4, and 5 represent spectra from four selected areas in **D**. Bars: 10 μ m

with PBS (pH 7.0) to get rid of any bacteria bound to its surface, was used for RNA isolation and qRT-PCR analysis, which targeted bacterial 16 S rRNA gene expression using the single-cell qRT-PCR method developed by our group. For qRT-PCR analysis, we analyzed three cells at each time point and five technical replicates for each single macrophage cell (i.e., the cDNA template from each cell was divided equally among the five PCR tubes). *E. coli* cDNA obtained from the bulk cells was also diluted to a similar level and used as a positive control. In general, very good reproducibility was achieved; the average data are reported in Fig. 6. The results showed that the expression of the 16 S rRNA gene can be detected 2 min after bacterial infection (Fig. 6), suggesting that the bacteria have been engulfed by the macrophages by that point in time. This result was consistent with the results of the confocal microscopic analysis (Fig. 5). We also performed qRT-PCR for infected macrophages at different time points during the time course up to 120 min, and the results showed that 16 S rRNA gene expression was constant during this period (2–120 min after infection), suggesting that no more bacteria were engulfed after the first 20 min. This is consistent with the results of the time-lapse confocal image analysis, where the fluorescent intensity from the sensor reached its peak at around 15–20 min, suggesting that uptake of bacteria by macrophages is a very fast biological process. In addition, no significant decrease in the 16 S rRNA gene expression level

was observed 120 min after infection, suggesting that the bacteria and their 16 S rRNA could still be intact. These results were also confirmed by plate recovery and bacterial counting (data not shown). However, it is worth noting that although we thoroughly washed the infected macrophages three times with PBS, a few of the surface-attached bacteria may not have been removed, in which case they would have contributed to the gene expression measurements in the single-cell RT-PCR approach.

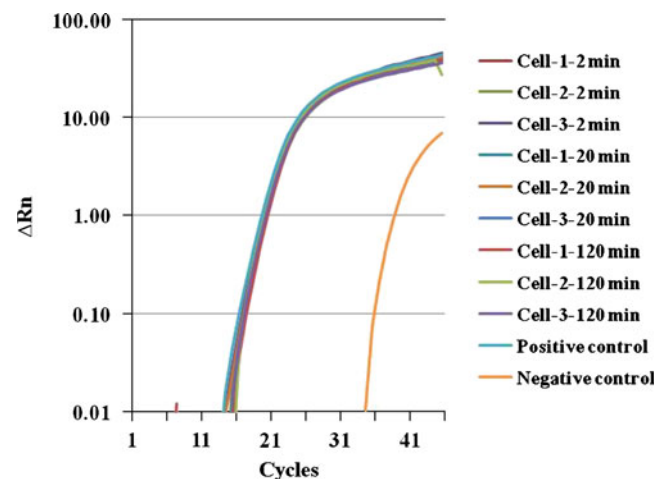


Fig. 6 Single-cell qRT-PCR analysis of bacterial infection of murine macrophage RAW 264.7

Discussion

A new TCF-containing pH sensor was synthesized and used to track bacterial infections of murine macrophages. The sensor emitted within the red spectral window. It exhibited weak fluorescence in neutral and basic aqueous solutions and strong emission under acidic conditions with a pK_a of 5.86. The sensor was also shown to be able to permeate into *E. coli*, *Bacillus*, and macrophage RAW 264.7 cells, and to act as lysosomal sensor for eukaryotic macrophage cells. A toxicity assay showed that the pH sensor exerts no significant effects on *E. coli* or murine macrophages. Time-lapse confocal image analysis showed that the sensor is sensitive enough to monitor the entry of bacteria into murine macrophages.

While most of the studies in this area have focused on the late stages of the bacteria–macrophage interaction [9, 35], we used pH sensor M to monitor the early stages of the entry of bacteria into macrophages and the bacteria–host interaction during phagocytosis. Although studies with *B. anthracis* spores suggested that a considerable percentage of the spores are killed soon after they have been taken up by macrophage vacuoles [35–37], our study using single-cell qRT-PCR suggested that most of the bacteria are still intact 120 min after infection. It may be worth investigating whether this is a species-specific response. The results also revealed that bacterial entry occurred quickly and could reach a plateau within several minutes, consistent with the results of an earlier study performed using lipophilic dye PKH-2 labeled *Listeria monocytogenes* and *Salmonella typhimurium* [38].

Using the pH sensor M, we were able to perform time-lapse monitoring of cell infection and to observe the real-time uptake of bacteria by macrophages. The results showed significant heterogeneity among murine macrophages in terms of bacterial engulfment. This finding is consistent with an early study on the uptake of fluorescently labeled *B. anthracis* spores by macrophages, which used flow cytometry to reveal extensive heterogeneity in terms of how RAW264.7 cells interact with *B. anthracis* spores [35]. Cell heterogeneity in terms of response to bacterial infection is an interesting and important topic, and is currently poorly understood [35, 39]. The novel pH sensor reported here could be a very useful tool for future research on this topic.

Finally, flow cytometry, especially when combined with fluorescence quenching, has been used to evaluate macrophage binding and the uptake of prelabeled bacteria [35, 38]. Although not tested directly in this study, we believe that, given its negligible inhibitory or toxic effects on bacteria and macrophages, pH sensor M can be used in conjunction with flow cytometry to concurrently discriminate between infected and uninfected macrophages.

Acknowledgement We would like to thank Dr. Weimin Gao for helping with single-cell qRT-PCR analysis and Dr. Yasser Anis for aiding the single-cell selection. This work was supported by the National Institutes of Health, Centers of Excellence in Genomic Science: Microscale Life Sciences Center (MLSC), grant #P50-HG002360 (PI, D. Meldrum).

References

1. Raybourne RB, Bunning VK (1994) *Infect Immun* 62:665–672
2. Falkow S, Isberg RR, Portnoy DA (1992) *Annu Rev Cell Biol* 8:333–363
3. Oh YK, Straubinger RM (1996) *Infect Immun* 64:319–325
4. Fields PI, Swanson RV, Haidaris CG, Heffron F (1986) *Proc Natl Acad Sci USA* 83:5189–5198
5. Conlan JW, North RJ (1992) *Infect Immun* 60:951–957
6. Guidi-Rontani C, Levy M, Ohayon H, Mock M (2001) *Mol Microbiol* 42:931–938
7. Dixon TC, Fadl AA, Koehler TM, Swanson JA, Hanna PC (2000) *Cell Microbiol* 2:453–463
8. Valdivia RH, Hromockyj AE, Monack D, Ramakrishnan L, Falkow S (1996) *Gene* 173:47–52
9. Ruthel G, Ribot WJ, Bavari S, Hoover TA (2004) *J Infect Dis* 189:1313–1316
10. Donnelly CW, Baiegant GJ (1986) *Appl Environ Microbiol* 52:689–695
11. Buchmeier NA, Heffron F (1989) *Infect Immun* 57:1–7
12. Haugland RP (2001) *Handbook of fluorescent probes and research chemicals*, 8th edn. Molecular Probes, Eugene
13. Oh DJ, Lee GM, Francis K, Palsson BO (1999) *Cytometry* 36:312–318
14. Clemens DL, Horwitz MA (2007) *Ann NY Acad Sci* 1105:160–186
15. Porte F, Liautard JP, Köhler S (1999) *Infect Immun* 67:4041–4047
16. Huynh KK, Grinstein S (2007) *Microbiol Mol Biol Rev* 71:452–462
17. Molenaar D, Bolhuis H, Abee T, Poolman B, Konings WN (1992) *J Bacteriol* 174:3118–3124
18. Whitaker JE, Haugland RP, Ryan D, Hewitt PC, Haugland RP, Prendergast FG (1992) *Anal Biochem* 207:267–275
19. Peng J, He X, Wang K, Tan W, Wang Y, Liu Y (2007) *Anal Bioanal Chem* 388:645–654
20. Abbotto A, Beverina L, Manfredi N, Pagani GA, Archetti G, Kuball HG, Wittenburg C, Heck J, Holtmann J (2009) *Chem Eur J* 15:6175
21. Lord J, Conley NR, Lee HLD, Samuel R, Liu N, Twieg RJ, Moerner WE (2008) *J Am Chem Soc* 130:9204
22. Bouffard J, Kim Y, Swager TM, Weissleder R, Hilderbrand SA (2008) *Org Lett* 10:37
23. Liu S, Haller MA, Ma H, Dalton LR, Jang SH, Jen AKY (2003) *Adv Mater* 15:603
24. Zheng S, Leclercq A, Fu J, Beverina L, Padilha LA, Zojer E, Schmidt K, Barlow S, Luo J, Jiang SH, Jen AKY, Yi Y, Shuai Z, Van Stryland EW, Hagan DJ, Bredas J, Marder SR (2007) *Chem Mater* 19:432
25. Louis B, Rose-Marie L, Minh L, Michel V (1995) *New J Chem* 19:141
26. Choi D, Song S, Lim SJ, Park SY, Kim N (1995) *Mol Cryst Liq Cryst* 267:53
27. Kubin RF, Fletcher AN (1982) *J Lumin* 27:455
28. Sambrook J, Russell D (2001) *Molecular cloning: a laboratory manual*. Cold Spring Harbor Laboratory, Cold Spring Harbor

29. Anis YH, Holl MR, Meldrum DR (2008) In: Proc 4th IEEE Conf on Automation Science and Engineering, Washington, DC, USA, 23–26 Aug 2008
30. Ramachandram B, Samanta A (1998) *J Phys Chem A* 102:10579
31. Ramachandram B, Saroja G, Sankaran B, Samanta A (2000) *J Phys Chem B* 104:11824
32. Valeur B (2002) *Molecular fluorescence: principles and applications*. Wiley, New York
33. Niu CG, Zeng GM, Chen LX, Shen GL, Yu RQ (2004) *Analyst* 129:20
34. Niu CG, Gui XQ, Zeng GM, Yuan XZ (2005) *Analyst* 130:1551
35. Stojkovic B, Torres EM, Prouty AM, Patel HK, Zhuang L, Koehler TM, Ballard JD, Blanke SR (2008) *Appl Environ Microbiol* 74:5201–5210
36. Hu H, Emerson J, Aronson AI (2007) *FEMS Microbiol Lett* 272:245–250
37. Hu H, Sa Q, Koehler TM, Aronson AI, Zhou D (2006) *Cell Microbiol* 8:1634–1642
38. Raybourne RB, Bunning VK (1994) *Infect Immun* 62:665–672
39. Ramsey S, Ozinsky A, Clark A, Smith KD, de Atauri P, Thorsson V, Orrell D, Bolouri H (2006) *Phil Trans R Soc Lond B* 361:495–506